Wat. Res. Vol. 27, No. 7, pp. 1119–1126, 1993
Printed in Great Britain.

0043-1354/93 $6.00 + 0.00

INTERACTIONS OF 1 μm LATEX PARTICLES WITH *PSEUDOMONAS AERUGINOSA* BIOFILMS

WILLIAM J. DRURY†, WILLIAM G. CHARACKLIS and PHILIP S. STEWART*
Center for Interfacial Microbial Process Engineering, Montana State University, 409 Cobleigh Hall, Bozeman, MT 59717-0398, U.S.A.

(First received July 1992; accepted in revised form January 1993)

Abstract—Fluorescently labelled latex microbeads were used to study the interaction of particles with *Pseudomonas aeruginosa* biofilms in a continuous flow annular reactor. Beads were readily distinguished and enumerated in both intact and disaggregated biofilm samples. The fraction of beads that attached to biofilm during a 24 h period ranged from 0.001 to 0.01 and was proportional to biofilm cell carbon and to the standard deviation of biofilm thickness. Microbeads added to biofilm of steady state thickness (30 μm) were observed to be located throughout the entire biofilm depth in 24 h. Many of the microbeads that attached to biofilm shortly after bacterial inoculation (thickness of 2 μm) remained near the substratum as cells grew past and covered them. Microbeads were observed near the biofilm–substratum interface for up to 5 days after bead addition. Beads formed aggregates on biofilms, but not in bulk water. Beads captured by biofilm remained in the reactor system longer than beads that never attached to biofilm.

Key words—biofilm, particle, microbead, bead, colloid, residence time, biofilm properties, *Pseudomonas aeruginosa*, attachment

INTRODUCTION

A biofilm has been defined as a film consisting of cells immobilized at a substratum and frequently embedded in an extracellular organic polymer (EPS) matrix of microbial origin. Biofilms may contain inorganic particles, such as clays, silts and corrosion products, or organic colloids, all of which are retained by the EPS matrix. Microorganisms and EPS may themselves be viewed as particulate constituents of the biofilm. Interactions between particles and biofilms represent processes that affect biofilm structure, chemistry and ecology significantly.

One important particle–biofilm interaction is the capture of particles from the bulk liquid. For example, the filamentous surface of a rotating biological contactor (RBC) biofilm entrapped particles such as organic solids (Alleman *et al.*, 1982). Reactor geometry influences particle capture by biofilms because it affects the surface area available for deposition of solids by gravity or interception of particles in the bulk flow (Bouwer, 1987). Biofilm grown on granular activated carbon (GAC) improved the capture of colloidal particles over clean GAC (Sprouse and Rittmann, 1990). Many substrates in natural systems exist as colloidal particles (Levine *et al.*, 1985). Capture of such substrates could increase biofilm growth over that produced by soluble substrates alone. Particle capture by biofilms may also improve the efficiency of sand filters. Capture of suspended bacteria could introduce new species to a biofilm.

Inorganic particles may be captured by or formed in biofilms. Corrosion products are examples of particles produced within a biofilm by microbially influenced corrosion. Inorganic corrosion products include FeS, $Fe(OH)_2$, $CaCO_3$ and elemental sulfur (Starkey, 1985). $Fe(OH)_2$ and sulfur are corrosive to steel, and FeS is cathodic to metallic iron and increases corrosion (Starkey, 1985; Tiller, 1985). Iron tubercles form in aerobic systems due to the dissolution of iron by iron oxidizing bacteria (Tiller, 1985). Since particulate corrosion products affect the corrosion process, knowledge of their location and rate of movement is an important aspect of understanding microbially influenced corrosion.

Inorganic particles can also be formed by chemical precipitation. Such particles were found in biofilms grown on swine wastes after 4–12 months of growth (Harvey *et al.*, 1984; Robinson *et al.*, 1984). Energy dispersive X-ray analyses revealed the precipitates to be composed mostly of calcium and phosphorus. It was assumed that the precipitates formed in the biofilms and were not captured from the bulk liquid because of their presence on the substratum and surrounding some bacterial cells.

Biofilm structure and function may be altered by a change in population dynamics caused by the capture of microbial species new to a biofilm. The previously-dominant species may become replaced by a species recently attached to the film. Particle movement in biofilms reflects competition for space by microbes,

*Author to whom all correspondence should be addressed.
†Present address: Environmental Engineering and Natural Sciences Division, Montana College of Mineral Sciences and Technology, Butte, MT 59701, U.S.A.

which may be important in biofilms (Atlas and Bartha, 1981). Some locations, such as near the substratum, have a special significance in population dynamics (Wanner, 1989). Therefore, shifts in population dynamics may be indicated by the change of the locations occupied by microbial cells. However, making observations on processes such as particle movement in intact biofilm is difficult (Gujer and Wanner, 1990).

The goal of this research was to investigate particle–biofilm interactions in a well-characterized model system. One objective was to develop an experimental system that allowed detailed analysis of these interactions. A technique was required to differentiate particles from bacterial cells, determine spatial and temporal distribution particles in biofilms, and permit quantification of particle concentrations in biofilm and bulk water. A second objective was to demonstrate capture and retention of micron-sized particles by biofilm. Fluorescently-labeled latex microbeads and a monopopulation *Pseudomonas aeruginosa* biofilm were used to meet these objectives.

MATERIALS AND METHODS

Experimental system

Biofilms were grown in a rotating annular reactor (RotoTorque) under turbulent flow conditions. The reactor has been described previously (Siebel and Characklis, 1991). It consists of a stationary outer cylinder and a rotating inner cylinder, both made of polycarbonate. The outer cylinder has twelve removable slides set in dove-tailed grooves so that biofilm samples can be removed periodically. The bulk fluid in the vessel is well mixed, so the reactor can be modeled as a continuous-flow stirred tank reactor. The rotation rate of the inner cylinder in these experiments was 200 rpm, producing a turbulent flow regime with a Reynolds number of 120,000 based on the annular gap width. The wetted surface area was 0.19 m^2, with a liquid volume of 5.75×10^{-4} m^3 at 200 rpm.

Reactor inoculation and operation

The reactor, attached tubing and dilution water filters were sterilized in an autoclave for 0.33 h. Two 0.011 m^3 Nalgene bottles containing concentrated mineral salts and phosphate buffer were autoclaved for 3.3 h, after which glucose was added to one of the bottles after filter sterilization through a 0.22 μm filter. Dilution water was sterilized by passage through two 0.2 μm capsule filters (Gelman No. 12122) in series.

The flow rate through the reactor was 2.3×10^{-3} m^3h^{-1}, producing a hydraulic retention time of 0.25 h. The reactor was partially immersed in a temperature-controlled water bath (25 ± 1°C) to maintain a constant temperature in the system. To initiate an experiment, a sterile reactor was inoculated with effluent from a chemostat for 12 h. The dilution rate of the chemostat was 0.12 h^{-1}, resulting in a *P. aeruginosa* concentration 5–7 $\times 10^{13}$ cells m^{-3}, and a delivery rate of 4.2×10^9 cells h^{-1}.

Microorganism and medium

Monopopulation biofilms of a *Pseudomonas aeruginosa* strain were grown in all experiments. This bacterium is a Gram-negative, motile rod-shaped chemoorganotroph (Palleroni, 1984). It is an obligate aerobe. Bacteria were grown aerobically on a defined mineral salts, phosphate buffered medium (Table 1). Glucose was the limiting nutrient and the sole carbon and energy source.

Table 1. Medium composition. All concentrations are in g m^{-3}. The final pH is 6.8

Compound	Concentration
Glucose	15
NH_4Cl	7.2
$MgSO_4 \cdot 7H_2O$	2.0
$(NH_4)_6Mo_7O_{24} \cdot 4H_2O$	0.001
$ZnSO_4 \cdot 7H_2O$	0.1
$MnSO_4 \cdot H_2O$	0.008
$CuSO_4 \cdot 5H_2O$	0.002
$Na_2B_4O_7 \cdot 10H_2O$	0.001
$FeSO_4 \cdot 2H_2O$	0.112
$(HOCOCH_2)_3N$	0.4
$CaCl_2 \cdot 2H_2O$	11.0
Na_2HPO_4	213
KH_2PO_4	204

Microbead characteristics

Microbeads (Polysciences Inc., No. 15702) were chosen to simulate the physical characteristics of a bacterial cell. They had the following properties: (1) a nominal diameter of 1 μm; (2) a specific gravity of 1.05; and (3) a negative surface charge due to the incorporation of carboxyl groups during bead manufacture. The microbeads contained a fluorescent dye, which made them easy to distinguish under the microscope. The beads were autoclaved for 0.33 h before their addition to the reactor.

Analytical methods

Reactor effluent (an 80 ml grab sample of 2 min duration) and biofilm (scraped area in the range of 19.6–32.3 cm^2) were sampled at 24 h intervals. Wet biofilm thickness was normally measured by the optical method of Bakke and Ollsen (1986), with from 5 to 10 measurements made per sample. For two samples in Experiment B-1, thickness was measured by a volumetric displacement method (van der Wende, 1991), which produces an average film thickness in one measurement with no measure of variation in film thickness. Microbead concentrations per unit surface area were determined from resuspended, homogenized biofilm samples by total direct counts and converted to suspended solids using the mean microbead diameter and specific gravity reported by the manufacturer.

Biofilm samples from Experiments A-1, B-2 and B-3 were fixed, embedded and cross-sectioned for microscopic examination. Polycarbonate membranes (approx. 0.028 × 0.012 m) were taped to some RotoTorque slides. After the slides with the membrane sections were removed from the reactor, the biofilm–membrane specimens were fixed in 2.5% glutaraldehyde, dehydrated in an ethanol series and embedded in JB-4 Plus plastic (Polysciences Inc.). Thin cross-sections (2.5 μm) were cut with a microtome and stained with Giemsa stain. The thin sections were examined and photographed with an Olympus BH-2 microscope using simultaneous transmitted white and epifluorescent light. Distance measurements on the thin cross-sections were made with the Olympus microscope and an American Innovision Videometric 150 image analysis system.

While there was no indication that artifacts were introduced by the protocol for the preparation of samples for microscopy, these cannot be ruled out. Never was there evidence of a track or tear in the sections indicating that a bead had been displaced during sectioning. A control of bead stability was performed in which beads were embedded in plastic and sectioned with a microtome. The beads appeared to be unaffected by the procedure, as judged by microscopic examination. According to the manufacturer, the beads are unaffected by glutaraldehyde.

Microbead aggregation in biofilm and bulk water was assessed using the Hopkins statistic nearest-neighbor analysis for clustering (Jain and Dubes, 1988). Four treated

Table 2. Experimental protocols

Experiment	Initiation of bead addition*	Length of bead addition period (h)	Total experiment duration (h)	Bulk liquid bead concentration during bead addition (No. m^{-3})	Fraction of beads which attached
A-1 (nascent)	0	24	144	3.9×10^{13}	0.0013
A-2 (nascent)	0	24	144	8.9×10^{12}	0.0038
B-1 (mature)	120	24	264	3.9×10^{12}	0.012
B-2 (mature)	120	24	264	2.9×10^{12}	0.010
B-3 (mature)	120	0.14	216	7.2×10^{14}	0.100

*Hours after the end of bacterial inoculation.

samples and one no-treatment control (beads without reactor effluent) were analyzed for bead aggregation in the bulk water. Clean microbeads were mixed with RotoTorque effluent for 0.25 h (one residence time in the reactor), then filtered on to a 0.2 μm membrane filter. The filters were observed microscopically with u.v. light, and bead locations were determined in a Cartesian coordinate frame with the image analysis system. Hopkins statistics were determined for ten fields per filter, with the ten values from each filter being averaged. Hopkins statistics were similarly determined for two biofilm samples. These samples were observed by phase contrast microscopy, with coordinates determined for a total of three fields.

RESULTS

The interaction of microbeads with biofilm was studied in two experimental designs. Microbeads were added to either nascent (Type A Experiments) or mature (Type B Experiments) biofilms. Nascent biofilms were thin (approx. 2 μm) with only partial surface coverage, while mature biofilms had reached maximum thickness (approx. 35 μm) with complete surface coverage. The biofilm reactor was operated for 96–120 h after the end of bead addition, during which time the biofilm was sampled to determine the number and distribution of beads in the biofilm. Experimental protocols are summarized in Table 2. Beads were added in a step up–step down pattern of 24 h duration (Experiments A-1, A-2, B-1 and B-2) or in a 0.14 h pulse (Experiment B-3).

Microbeads added in aqueous suspension to the reactor attached to the biofilm. The fractions of attaching microbeads ranged from 10^{-3} to 10^{-1} and are reported in Table 2. The fractions were calculated as the number of microbeads attached to biofilm at the end of the bead addition period divided by the number of beads pumped into the reactor. Very few beads attached when added to a sterile reactor. The attaching fraction in this control experiment was less than about 10^{-5}.

Individual microbeads attached to biofilm were readily identified and distinguished from bacteria. Section views indicate the presence of beads in the biofilm (Fig. 1). Beads can be identified at relatively low magnification (125×) when fluorescing, giving sensitivity to the identification and counting process. Counting of individual beads directly on the slides (plan view) was not always possible because of the presence of bead aggregates.

Microscopic examination of the thin cross-sections from the nascent biofilm Experiment A-1 indicated that microbeads were located near the substratum at

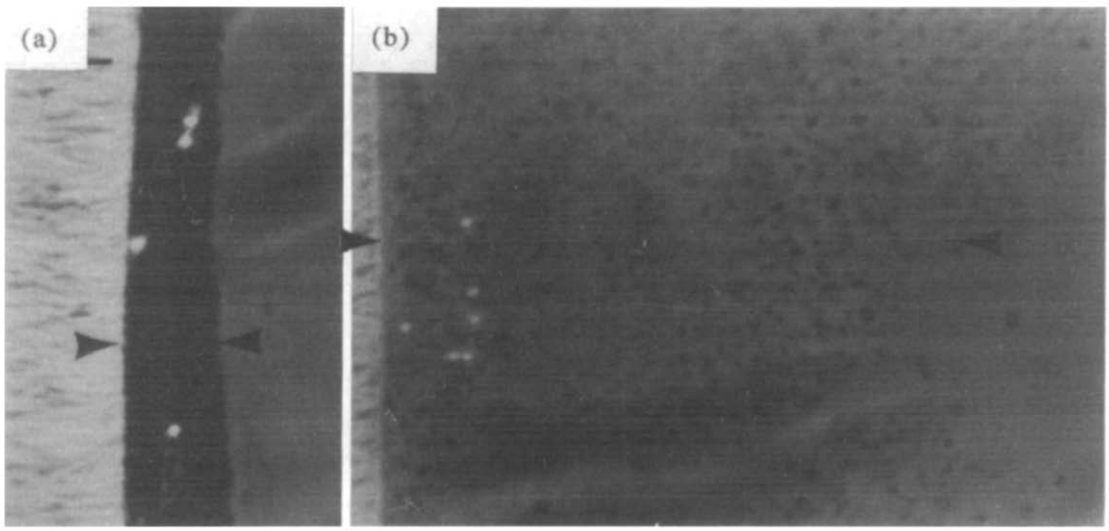

Fig. 1. Biofilm cross-sections from Experiment A-1. Arrowheads indicate the extent of the biofilm. The substratum is on the left. (a) Section from 48 h after the end of bacteria inoculation. The bacteria (dark particles) have grown over and entrapped the microbeads (light particles). (b) Section from 144 h. The remaining microbeads were generally located near the substratum. Bar = 5 μm.

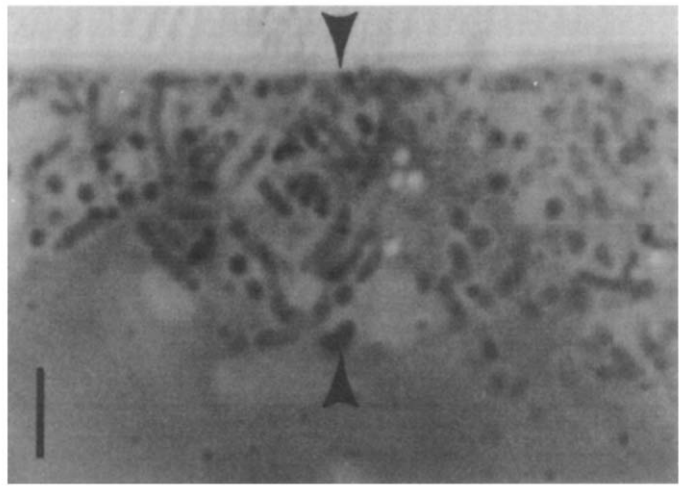

Fig. 2. Biofilm cross-section from 144.75 h in Experiment B-2. The sample was taken 45 min after the cessation of microbead addition. Microbeads had effectively penetrated the entire biofilm thickness. Bar = 5 μm.

48 and at 144 h after the end of bacterial inoculation (Fig. 1). Microbeads were predominantly nearer to the substratum than to the bulk water surface.

Thin sections from the mature biofilm Experiment B-2 show microbeads located throughout the depth of the biofilm 0.75 h after the end of microbead inoculation (Fig. 2). Most of the microbeads were located near the biofilm–bulk water interface shortly after bead addition. Later in the experiment, the majority of the beads that remained in the biofilm were near the substratum.

Thin sections from the mature biofilm Experiment B-3 (pulse bead addition) show that beads were associated primarily with the biofilm–bulk water interface immediately after bead addition. The biofilm surface was irregular, with pores or crevices. The pores usually contained beads [Fig. 3(a) and (b)]. At 8.9 h after bead addition, several layers of bacteria

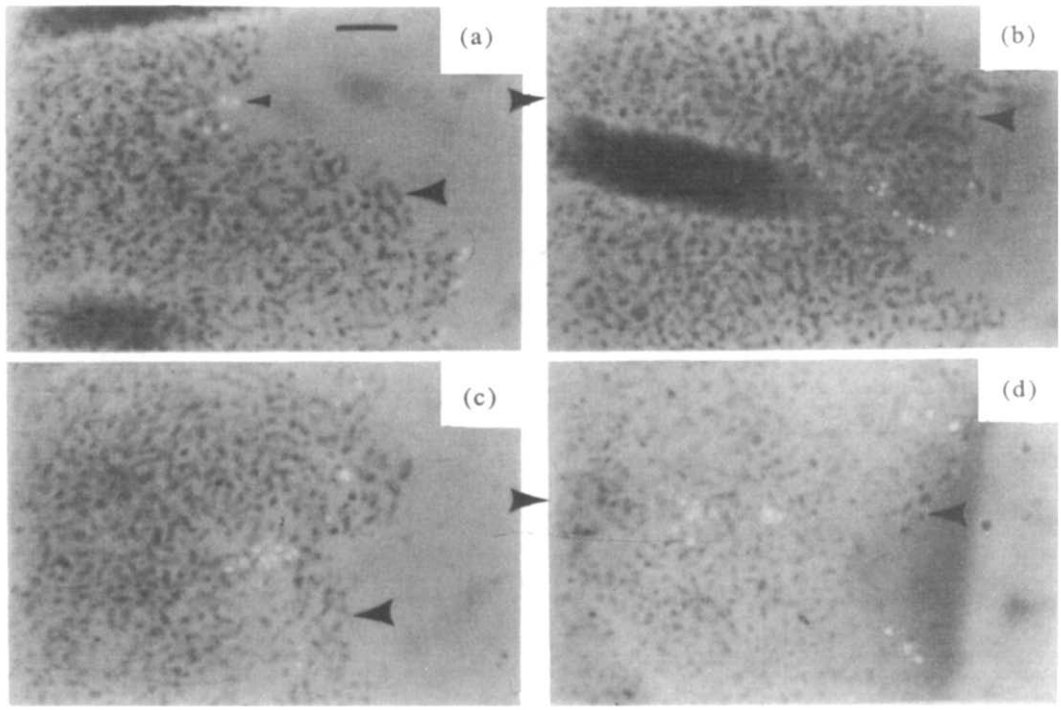

Fig. 3. Biofilm cross-sections from Experiment B-3. (a) At 120.05 h, microbeads are at the biofilm–bulk water interface, including pore interfaces. Small arrowhead = bead; large arrowhead = biofilm surface. Bar = 5 μm. (b) Also at 120.05 h, another view of how pores provide a conduit for particle movement into a biofilm. (c) Microbeads are in the interior of the biofilm and not associated with an interface at 128.9 h. (d) Much of the biofilm thickness contains microbeads at 143.9 h. The dark areas in (a) and (b) are wrinkles produced during manufacture of the cross sections.

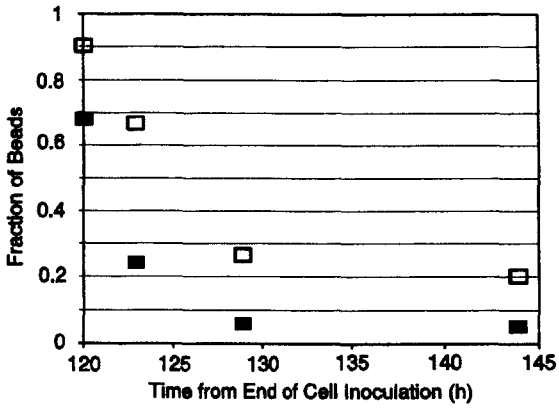

Fig. 4. Fractions of microbeads located at (■) and within 3 μm (□) of the biofilm–bulk water interface over the first 24 h after bead addition in Experiment B-3.

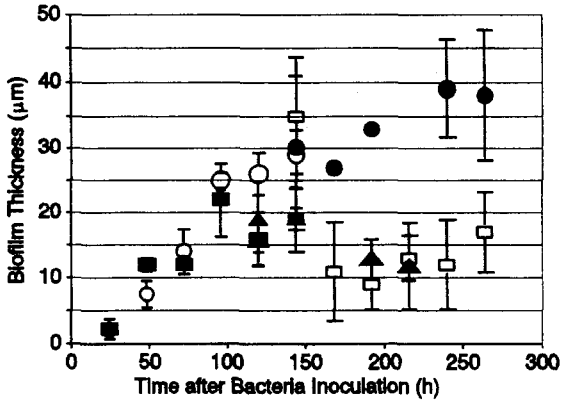

Fig. 6. Biofilm thickness over time in the nascent and mature biofilm experiments. The thicknesses are the mean of several measurements. The error bars represent 1 SD of the measurements. The two points with no standard deviations reported represent measurements by the volumetric displacement method. Experiment A-1: ○; A-2: ■; B-1: ●, B-2: □; and B-3: ▲.

covered most of the beads [Fig. 3(c)]. Beads were located even farther away from the biofilm–bulk water interface as time progressed [Fig. 3(d)].

The fractions of beads at the biofilm–bulk water interface decreased rapidly in the first 3 h after bead addition in Experiment B-3 (Fig. 4). This decrease continued at a lesser rate for the next 21 h. The numbers of beads within 3 μm of the biofilm–bulk water interface decreased in a similar pattern.

Biofilm microbead concentrations decreased over time. The progression of microbead concentrations in Experiments A-1, A-2, B-1 and B-2 is presented in Fig. 5. Data for Experiment B-3 are not shown, since those concentrations are an order of magnitude greater than the concentrations for the other experiments.

Biofilm thicknesses for the nascent and mature biofilm experiments are shown in Fig. 6. Biofilm thickness measured at distinct points on a given sample vary significantly, suggesting a three-dimensional biofilm structure that includes pores or ridges. A putative pore is shown in a scanning confocal laser microscope image of a specimen from Experiment A-2 (Fig. 7). The pore is approx. 50 μm in diameter.

With the Hopkins statistic, a value of 0.5 represents a random distribution of points, while values near 1.0 indicate that aggregation has occurred. The Hopkins statistic values for all bulk liquid samples, including the control, were approx. 0.6, with standard deviations in the ten analyses per filter ranging from 0.059 to 0.14. Because the statistics are near 0.5 and statistics for the treated samples equal that of the control, no bead aggregation occurred in these tests.

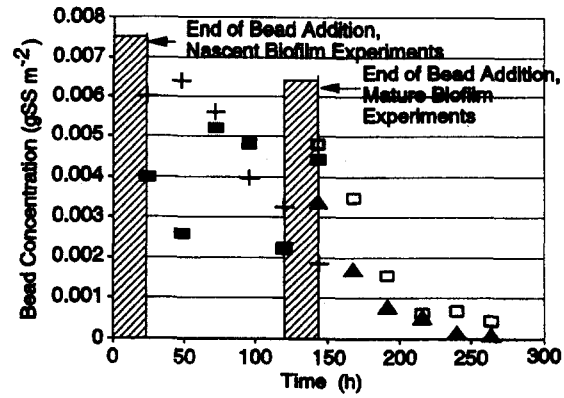

Fig. 5. Biofilm microbead concentrations vs time for the nascent (■, +) and mature (□, ▲) biofilm experiments.

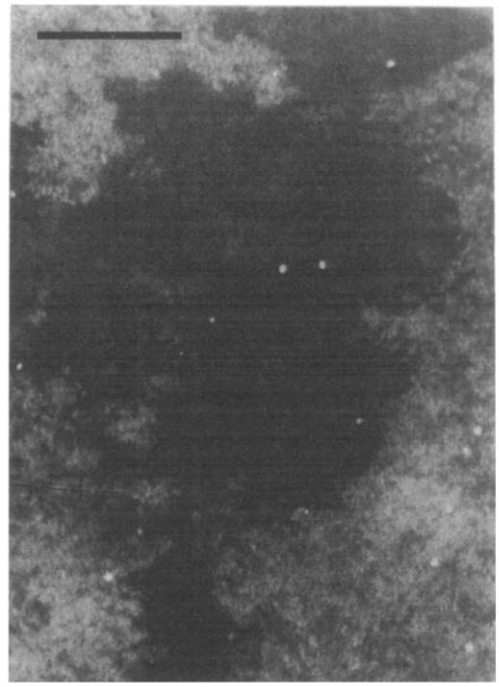

Fig. 7. A photomicrograph taken by a scanning confocal laser microscope of a biofilm sample taken at 142 h in Experiment A-2. A pore, representing a large variation in biofilm thickness, is evident in the center of the image. Microbeads were located in areas of thick and thin biofilm.

However, the biofilm samples had Hopkins statistic values ranging from 0.93 to 0.98. Therefore, beads did aggregate in or on the biofilm.

DISCUSSION

Fluorescent latex microbeads have been shown to be effective tracers for particle movement in biofilms. They were easily differentiated from bacterial cells when viewed under a microscope, whether or not the beads were fluorescing. Microbead locations could be determined in both plan and section views. Microbead concentrations in biofilm were quantifiable.

Microbead attachment

The fraction of attaching microbeads was proportional to the quantity of biofilm present during the attachment period (Fig. 8). Both the amount of biofilm present at the ends of the 24 h attachment period and the fraction of attaching microbeads in the nascent biofilm experiments were approximately one order of magnitude less than in the mature biofilm experiments (Fig. 8). This result is consistent with the observations that microbeads (J. Bryers, personal communication) and bacterial cells (Banks and Bryers, 1992) attach to biofilm at higher rates than to a clean glass surface. It also agrees with the observations of Rittmann and Wirtel (1991), who reported the removal of 1 μm diameter milk colloids in a fluidized bed, granular activated carbon biofilm reactor to increase from 87.4 to 91.5% when the amount of biofilm increased from 0.134 to 1.74 mg cellular carbohydrate per gram of dry carbon. The attachment fractions for beads were comparable to the 0.03–0.06 measured for *P. aeruginosa* cells attaching to a *P. aeruginosa* biofilm in a RotoTorque (Gunawan, 1991). The attachment fraction in Experiment B-3 (0.100) was higher than in the other mature biofilm experiments. This could have occurred due to attached microbeads detaching before quantification in Experiments B-1 and B-2. Another possibility for this difference is that the higher bead concentration in the bulk water during bead addition in Experiment B-3 (200 times, Table 2) resulted in greater attachment or retention than occurred in the other mature biofilm experiments.

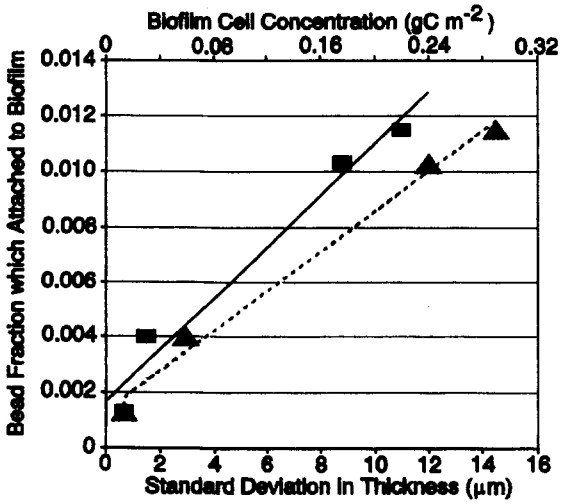

Fig. 8. Fraction of microbeads attached to the biofilm versus biofilm cell carbon (■,——) and standard deviation in thickness (▲,---). The fraction that attached was directly proportional to the amount of biomass and the variation in thickness.

The microbead fraction that attached to biofilm was also proportional to the standard deviation in biofilm thickness measurements (Fig. 8). The thickness variation in the mature biofilm experiments was greater than for the nascent biofilm experiments (Fig. 6). A similar increase in thickness standard deviation with biofilm age was reported by Bakke (1986), who found that the standard deviation of thickness measurements doubled between 50 and 300 h of growth for a *P. aeruginosa* film. Biofilms consisting of other bacterial species can have standard deviations in thickness larger than the standard deviations measured in this research (Siebel and Characklis, 1991; Eighmy *et al.*, 1983; Mack *et al.*, 1975). A larger variation in thickness represents more or deeper pores. Beads attached in pores may be retained for longer periods than beads at the exposed biofilm–bulk water surface. Beads attached in pores may be relatively protected from hydrodynamic shear stress, and less likely to detach than beads not in pores. Also, cell growth can fill in the pores and bury the beads, increasing their retention in the biofilm.

The fraction of beads which attached to biofilm was also proportional to biofilm thickness, but was correlated somewhat less strongly with biofilm thickness that with the variables represented in Fig. 8. The least squares correlation coefficient (r^2) was 0.99 for biofilm cell carbon, 0.97 for standard deviation in biofilm thickness and 0.91 for biofilm thickness. Whatever the measure, these data indicate that bead capture and retention increases with an increasing amount of biofilm.

Microbead distribution

The existence of pores in biofilms provides a possible mechanism for biofilms to envelop cells and particles. Pores were observed in the biofilms grown in these experiments (Fig. 7). Electron microscopic observations of biofilms and sludge granules have shown rough surfaces with interiors penetrated by pores. Switzenbaum and Eimstad (1987) examined anaerobic biofilms from biological filters and fluidized beds, and reported the films to be uneven, containing ridges, holes and channels. Eighmy *et al.* (1983) reported the existence of channels in biofilms which markedly increased the biofilm surface area. The bacteria in the films appeared to be aggregated and did not reside in contiguous layers. Robinson *et al.* (1984) observed biofilms from anaerobic fixed film reactors, which contained rough and uneven surfaces, with "volcano-like" structures penetrating

the films. Openings and channels throughout the films were common. Mack *et al.* (1975) observed "slit-like" openings in trickling filter biofilms. Cavities in bacterial aggregates have been reported (Beeftink and Staugaard, 1986; MacLeod *et al.*, 1990; Bochem *et al.*, 1982).

Deposition of particles in a random manner would place some beads in pores. Observations of the thin cross-sections (for example, Fig. 3) indicated that pores filled in with bacteria, burying any particles residing in the pores. Therefore, pores in the biofilms were probably short-lived with their creation causing a biofilm to capture particles and their disappearance leading to particle retention. The presence of beads in pores immediately after bead addition (Fig. 3) and the decreasing fraction of beads at the biofilm–bulk water interface (Fig. 4) indicated that bacteria covered the beads as the bacterial population increased.

Three possible explanations exist as to why the beads aggregated in or on the biofilm. Beads attached in pores may have been less likely to detach and, therefore, were more likely present when the photomicrographs for bead spatial analysis were obtained. This would give the appearance of aggregates having been formed in pores. Secondly, the probability of bead detachment may have been higher for individual beads than for bead aggregates, so that a relatively large amount of aggregates were present when the photomicrographs were taken. The third reason is that some beads aggregated on the biofilm surface during attachment because of a high affinity between beads. Our data are inadequate for determining which of these hypotheses are correct.

Biofilm ecology

These experiments with microbeads simulate the fate of quiescent microorganisms and demonstrate the ecological difference between biofilm and the bulk water associated with the biofilm. Quiescent microorganisms are microbes subsisting in a non-reproducing state brought on by nutrient starvation or other conditions (Lewis and Gattie, 1991; Lewis, 1991). Whereas suspended particles do not remain in the reactor environment for more than an hour (four hydraulic residence times), at least 10–30% of those beads that were attached when the bead concentrations were first quantified remained in the biofilms for 120 h. The large difference in particle retention times between biofilm and the bulk water means that particles in the biofilm have a better chance of being subjected to differing time-variable environmental conditions. The long retention time that can be experienced by quiescent microorganisms in biofilms provides a greater possibility that these microbes attain significant activity if the environment changes so that conditions are conducive for their replication.

Particle movement into biofilms has two other implications for biofilm dynamics. It indicates how anaerobic bacteria may move from oxygenated bulk water to the lower anaerobic layer of an oxygen-limited biofilm. For example, sulfate-reducing bacteria cannot grow in aerobic conditions, but they can be found in biofilms on the walls of pipes carrying aerated water. They could be transported to the anaerobic depths of the biofilm through pores in the biofilm. Also, particle transport into biofilms provides a mechanism for colloidal substrates to move deep into a biofilm and nourish microorganisms there.

CONCLUSIONS

(1) Fluorescent latex microbeads attach to biofilm and are easily identified and enumerated separately from bacteria.
(2) Biofilms are sufficiently porous for bacterial-sized latex particles to become entrapped in them. Tracer particles penetrated the full depth of a 34 μm *P. aeruginosa* biofilm.
(3) Microbead capture by biofilm was proportional to the biofilm cell carbon concentration and to the standard deviation in biofilm thickness measurements.
(4) Microbeads form aggregates on biofilms, but not in the associated bulk water.
(5) The retention time of microbeads in a biofilm was much longer than the retention time of suspended particles in the biofilm reactor.

Acknowledgements—The authors gratefully acknowledge support through Cooperative Agreement ECD-8907039 between the National Science Foundation and Montana State University and the Center Industrial Associates. The authors thank Gayle Callis for the preparation of the cross-sections and Gary Harkin for recommending and writing a computer program for the Hopkins statistic.

REFERENCES

Alleman J. E., Veil J. A. and Canaday J. T. (1982) Scanning electron microscope evaluation of rotating biological contactor biofilm. *Wat. Res.* **16**, 543–550.

Atlas R. M. and Bartha R. (1981) *Microbial Ecology: Fundamentals and Applications*. Addison–Wesley, Reading, Mass.

Bakke R. (1986) Biofilm detachment. Unpublished doctoral thesis, Montana State University, Bozeman, Mont.

Bakke R. and Ollsen P. Q. (1986) Biofilm thickness measurements by light microscopy. *J. Microb. Meth.* **5**, 1–6.

Banks M. K. and Bryers J. D. (1992) Microbial deposition rates onto clean glass and pure culture bacterial biofilm surfaces. *Biofouling* **6**, 81–86.

Beeftink H. H. and Staugaard P. (1986) Structure and dynamics of anaerobic bacterial aggregates in a gas lift reactor. *Appl. envir. Microbiol.* **52**, 1139–1146.

Bochem H. P., Schoberth S. M., Sprey B. and Wengler P. (1982) Thermophilic biomethanation of acetic acid: morphology and ultrastructure of a granular consortium. *Can. J. Microbiol.* **28**, 500–510.

Bouwer E. J. (1987) Theoretical investigation of particle deposition in biofilm systems. *Wat. Res.* **21**, 1489–1498.

Eighmy T. T., Maratea D. and Bishop P. L. (1983) Electron microscopic examination of wastewater biofilm formation and structural components. *Appl. envir. Microbiol.* **45**, 1921–1931.

Gujer W. and Wanner O. (1990) Modelling mixed population biofilms. In *Biofilms* (Edited by Characklis W. G. and Marshall K. C.), pp. 307–444, Wiley, New York.

Gunawan C. (1991) Rates of cellular attachment to an established biofilm. Unpublished master's thesis, Montana State University, Bozeman, Mont.

Harvey M., Forsberg C. W., Beveridge T. J., Pos J. and Ogilvie J. R. (1984) Methanogenic activity and structural characteristics of the microbial biofilm on a needle-punches polyester support. *Appl. envir. Microbiol.* **48**, 633–638.

Jain A. K. and Dubes R. C. (1988) *Algorithms for Clustering Data*. Prentice-Hall, Englewood Cliffs, N.J.

Levine A.D., Tchobanoglous G. and Asano T. (1985) Characterization of the size distribution of contaminants in wastewater: treatment and reuse implications. *J. Wat. Pollut. Control Fed.* **57**, 805–816.

Lewis D. L. (1991) Letters to the editor. *ASM News* **57**, 342.

Lewis D. L. and Gattie D. K. (1991) The ecology of quiescent microbes. *ASM News* **57**, 27–32.

Mack W. N., Mack J. P. and Ackerson A. O. (1975) Microbial film development in a trickling filter. *Microb. Ecol.* **2**, 215–226.

MacLeod F. A., Guiot S. R. and Costerton J. W. (1990) Layered structure of bacterial aggregates produced in an upflow anaerobic sludge bed and filter reactor. *Appl. envir. Microbiol.* **56**, 1598–1607.

Palleroni N. J. (1984) Genus I. *Pseudomonas*. In *Bergey's Manual of Systematic Bacteriology* (Edited by Krieg N. R.), Vol. 1, pp. 141–174. Williams & Wilkins, Baltimore, Md.

Rittmann B. R. and Wirtel S. A. (1991). Effect of biofilm accumulation on colloid cohesion. *J. envir. Engng* **117**, 692–695.

Robinson R. W., Akin D. E., Nordstedt R. A., Thomas M. V. and Aldrich H. C. (1984) Light and electron microscopic examinations of methane-producing biofilms from anaerobic fixed-bed reactors. *Appl. envir. Microbiol.* **48**, 127–136.

Siebel M. A. and Characklis W. G. (1991) Observations of binary population biofilms. *Biotechnol. Bioengng* **37**, 778–789.

Sprouse G. and Rittmann B. E. (1990) Colloidal removal in fluidized-bed biofilm reactor. *J. envir. Engng* **116**, 314–329.

Starkey R. L. (1985) Anaerobic corrosion—perspectives about causes. In *Biologically Induced Corrosion. Proceedings of the International Conference on Biologically Induced Corrosion* (Edited by Dexter S. C.), pp. 3–7. National Association of Corrosion Engineers, Houston, Tex.

Switzenbaum M. S. and Eimstad R. B. (1987) Analysis of anaerobic biofilms. *Envir. Technol. Lett.* **8**, 21–32.

Tiller A. K. (1985) A review of the European research effort on microbial corrosion between 1950 and 1984. In *Biologically Induced Corrosion. Proceedings of the International Conference on Biologically Induced Corrosion* (Edited by Dexter S. C.), pp. 8–29. National Association of Corrosion Engineers, Houston, Tex.

Wanner O. (1989) Modelling population dynamics. In *Structure and Function of Biofilms* (Edited by Characklis W. G. and Wilderer P. A.), pp. 91–110. Wiley, New York.

van der Wende E. (1991) Biocide action of chlorine on *Pseudomonas aeruginosa* biofilm. Unpublished doctoral thesis, Montana State University, Bozeman, Mont.